Pramana – J. Phys. (2016) 87: 63
DOI 10.1007/s12043-016-1269-8

Homotopy deform method for reproducing kernel space for nonlinear boundary value problems

MIN-QIANG XU* and YING-ZHEN LIN

School of Science, Zhuhai Campus, Beijing Institute of Technology, Zhuhai,
Guangdong, 519085, People's Republic of China
*Corresponding author. E-mail: mqxu_math@126.com

MS received 11 September 2015; revised 15 October 2015; accepted 16 December 2015; published online 23 September 2016

Abstract. In this paper, the combination of homotopy deform method (HDM) and simplified reproducing kernel method (SRKM) is introduced for solving the boundary value problems (BVPs) of nonlinear differential equations. The solution methodology is based on Adomian decomposition and reproducing kernel method (RKM). By the HDM, the nonlinear equations can be converted into a series of linear BVPs. After that, the simplified reproducing kernel method, which not only facilitates the reproducing kernel but also avoids the time-consuming Schmidt orthogonalization process, is proposed to solve linear equations. Some numerical test problems including ordinary differential equations and partial differential equations are analysed to illustrate the procedure and confirm the performance of the proposed method. The results faithfully reveal that our algorithm is considerably accurate and effective as expected.

Keywords. Nonlinear differential equations; the homotopy deform method; the simplified reproducing kernel method; Adomian decomposition method.

PACS Nos 02.30.Mv; 02.30.Tb

1. Introduction

The nonlinear equations, subject to given boundary conditions, have gained considerable attention due to their wide applications in applied mathematics, theoretical physics, engineering and so on. In fact, accurate and fast numerical solutions for nonlinear equations with BVPs are of great importance because of their wide applications in scientific and engineering research.

Investigations on the existence and uniqueness of the solution of the BVPs are given in [1–7]. Recently, because of the difficulties in finding exact analytical solutions as well as the development of the modern high-speed digital computers, the numerical algorithms of these problems have attracted more and more attention. Therefore, many new numerical algorithms have been proposed and applied successfully to approximate the nonlinear equations. Among these papers, Geng [8] presented a method for a class of second-order three-point BVPs by converting the original problem into an equivalent integro differential equation. Another was the convenient analytic recurrence algorithm for the Adomian polynomials by Duan [9]. Tatari and Dehghan [10] presented an algorithm for solving multipoint BVPs by the well-known Adomian decomposition method, while Geng and Cui [11] developed an algorithm for solving nonlinear multipoint BVPs by combining homotopy perturbation and variational iteration methods. Most recently, Duan and Rach [12] proposed a new modification of the Adomian decomposition method for solving BVPs for higher-order nonlinear differential equations. Meanwhile, Abbas and Mehdi [13] used the sinc-collocation method for solving multipoint boundary value problems.

In this paper, we are concerned with the numerical solution of the following nonlinear BVPs:

$$\begin{cases}\mathcal{A}(u) = f(\mathbf{X}), & u \in H,\ f(\mathbf{X}) \in \hat{H}, \mathbf{X} \in \Omega,\\ \mathcal{R}(u) = \alpha, & \alpha \in R^c,\end{cases} \tag{1}$$

where H and $\hat{H}$ are arbitrary real Hilbert spaces, $\mathcal{A}$: $H \to \hat{H}$ is a general differential operator, $\mathcal{R}$: $H \to R^c$ is a linear boundary operator, $\mathcal{R} = (\mathcal{R}_1, \mathcal{R}_2, \ldots, \mathcal{R}_c)$, $\alpha = (\alpha_1, \alpha_2, \ldots, \alpha_c)$ and f is a continuous function.

In our present work, using homotopy deform method [14], the nonlinear differential equation (1) can be converted to a series of linear BVPs. After that, the SRKM is presented to solve the linear differential equations. Different from the traditional RKM, there are many innovations in our method. One important improvement is that we successfully construct a novel reproducing kernel space so as to overcome difficulties with the various boundary value conditions. Because of this improvement, not only does the reproducing kernel has the uniformity which implies the reproducing kernel will stay consistent, but also the expression is extremely simple compared to the reproducing kernel presented in [15]. The expressions of the reproducing kernels are given as follows:

$$K_y^m(x) = \begin{cases} \displaystyle\sum_{i=0}^{m} \left(\frac{(y-a)^i}{i!} + (-1)^{m-1-i} \frac{(y-a)^{2m-1-i}}{(2m-1-i)!} \right) \\ \qquad \times \dfrac{(x-a)^i}{i!}, \quad x > y, \\ \displaystyle\sum_{i=0}^{m} \left(\frac{(x-a)^i}{i!} + (-1)^{m-1-i} \frac{(x-a)^{2m-1-i}}{(2m-1-i)!} \right) \\ \qquad \times \dfrac{(y-a)^i}{i!}, \quad y > x. \end{cases} \tag{2}$$

As known to all, the reproducing kernel can be applied in various calculations. This makes calculations much easier. Moreover, homogenization is not essential in our method. As far as the third improvement is concerned, the Schmidt orthogonalization process which requires a large number of calculations in every linear equation is less likely to be employed. Therefore, a reversible matrix is expected to be obtained, which will remain consistent in the series of linear equations. Compared to the RKM, the SRKM is more flexible and can reduce the amount of computations. It is shown that the SRKM is a remarkably efficient numerical algorithm for solving linear BVPs.

This paper is organized as follows. In §2, we present the homotopy deform method. In §3, we develop an algorithm for solving linear differential equation with BVPs. In §4, the proposed methods are applied to several examples. Section 5 ends this paper with a brief conclusion.

2. The homotopy deform method

Generally speaking, the operator $\mathcal{A}$ can be divided into a linear operator $\mathcal{L}$ and a nonlinear operator $\mathcal{N}$. Therefore, the differential eq. (1) can be rewritten as

$$\begin{cases} \mathcal{L}(u) + \mathcal{N}(u) - f(\mathbf{X}) = 0, & u \in H,\ f \in \hat{H}, \mathbf{X} \in \Omega, \\ \mathcal{R}(u) = \alpha, & \alpha \in R^c. \end{cases} \tag{3}$$

Next, we focus on the nonlinear operator $\mathcal{N}$. By the homotopy technique, we construct a homotopy function $u(\mathbf{X}, p)$: $\Omega \times [0, 1] \to R$ in reproducing kernel space W, and we define a homotopy function $H(u(\mathbf{X}, p), p)$: $W \times [0, 1] \to R$ as

$$\begin{aligned} H(u(\mathbf{X}, p), p) = {} & (1-p)(\mathcal{L}(u(\mathbf{X}, p)) - f(\mathbf{X})) \\ & + p(\mathcal{L}(u(\mathbf{X}, p)) - f(\mathbf{X}) \\ & + \mathcal{N}(u(\mathbf{X}, p))), \end{aligned} \tag{4}$$

where $p \in [0, 1]$ is an embedding parameter. By simplifying eq. (4), one can obtain

$$H(u(\mathbf{X}, p), p) = \mathcal{L}(u(\mathbf{X}, p)) - f(\mathbf{X}) + p\mathcal{N}(u(\mathbf{X}, p)).$$

Obviously, when p changes from 0 to 1, the homotopy function continuously deforms from $H(u, 0)$ to $H(u, 1)$. In fact, $H(u, 0) = 0$ gives the following equation:

$$\mathcal{L}(u) - f(\mathbf{X}) = 0.$$

$H(u, 1) = 0$ gives the following equation:

$$\mathcal{L}(u) - f(\mathbf{X}) + \mathcal{N}(u) = 0.$$

In this way, we obtain a method using homotopy deformation to solve the nonlinear differential equation.

The Taylor's expansion in $p = 0$ of the $u(\mathbf{X}, p)$ is:

$$u(\mathbf{X}, p) = \sum_{i=0}^{+\infty} \frac{\partial^i u(\mathbf{X}, 0)}{\partial p} p^i \triangleq \sum_{i=0}^{+\infty} u_i(\mathbf{X}) p^i. \tag{5}$$

Applying the method we proposed, one can get the solution $u(x)$ of eq. (3).

$$u(X) = \lim_{p \to 1} u(\mathbf{X}, p) = u_0(x) + u_1(x) + \cdots + u_k(x) + \cdots.$$

Substituting eq. (5) into $H(u(\mathbf{X}, p), p) = 0$ yields,

$$\sum_{i=0}^{+\infty} \mathcal{L}(u_i) p^i - f(x) + p\mathcal{N}\left(\sum_{i=0}^{+\infty} u_i p^i \right) = 0. \tag{6}$$

At the same time,

$$\mathcal{N}\left[\sum_{i=0}^{+\infty} u_i p^i\right] = \mathcal{N}(u_0) + \mathcal{N}'(u_0)p + \frac{1}{2!}[\mathcal{N}''(u_0)u_1^2 + 2\mathcal{N}'(u_0)u_2]p^2 + \cdots . \tag{7}$$

Substituting eq. (7) into eq. (6) yields

$$\sum_{i=0}^{+\infty} \mathcal{L}(u_i)p^i - f(t) + p(\mathcal{N}(u_0) + \mathcal{N}'(u_0)p + \frac{1}{2!}[\mathcal{N}''(u_0)u_1^2 + 2\mathcal{N}'(u_0)u_2]p^2 + \cdots) = 0. \tag{8}$$

Comparing the coefficients of p, we get the following equations:

$$\begin{aligned}
\mathcal{L}(u_0) &= f(x),\\
\mathcal{L}(u_1) &= -\mathcal{N}(u_0),\\
\mathcal{L}(u_2) &= -\mathcal{N}'(u_0)v_1,\\
\mathcal{L}(u_3) &= -\frac{1}{2!}[\mathcal{N}''(u_0)u_1^2 + 2\mathcal{N}'(u_0)u_2],\\
&\cdots\cdots\cdots\\
\mathcal{L}(u_k) &= -\frac{1}{(k-1)!}\frac{\mathrm{d}^{k-1}}{\mathrm{d}p^{k-1}}\left[\mathcal{N}\left(\sum_{i=0}^{+\infty} u_i p^i\right)\right]\Bigg|_{p=0},\\
&\cdots\cdots\cdots .
\end{aligned}$$

The nonlinear differential eq. (3) can be converted to a series of linear BVPs.

$$\begin{cases}\mathcal{L}(u_k) = f_k(\mathbf{X}), & u_k \in H,\ f \in \hat{H}, \mathbf{X} \in \Omega,\\ \mathcal{R}(u_k) = \alpha/2^{k+1}, & \alpha \in R^c,\end{cases} \tag{9}$$

for $k = 0, 1, \ldots,$ where

$$\begin{aligned}
f_0(x) &= f(x),\\
f_k &= -\frac{1}{(k-1)!}\frac{\mathrm{d}^{k-1}}{\mathrm{d}p^{k-1}}\left[\mathcal{N}\left(\sum_{i=0}^{k-1} u_i p^i\right)\right]\Bigg|_{p=0},\\
k &= 1, 2, \ldots .
\end{aligned}$$

All these equations are linear ones with the same form as follows:

$$\begin{cases}\mathcal{L}(u) = f(\mathbf{X}), & u \in H,\ f \in \hat{H}, \mathbf{X} \in \Omega,\\ \mathcal{R}(u) = \alpha, & \alpha \in R^c.\end{cases} \tag{10}$$

In §3, we put forward some new modifications of the reproducing kernel methods to solve the linear equations.

3. The simplified reproducing kernel method

In this section, we first introduce some basic concepts of the reproducing kernel. Then the SRKM is broached to solve the linear eq. (10).

DEFINITION 3.1 [16]

Let $\mathcal{H} = \{f(x) | f(x)$ is a real value function or complex function, $x \in A$, A is an abstract set$\}$ is a Hilbert space, equipped with inner product

$$\langle u(x), v(x)\rangle_{\mathcal{H}}, \quad u(x), v(x) \in \mathcal{H}.$$

If there exists a function $K_y(x)$, for each fixed $y \in A$, then $K_y(x) \in \mathcal{H}$, and any $u(x) \in \mathcal{H}$, which satisfies

$$\langle f(x), K_y(x)\rangle_{\mathcal{H}} = u(y),$$

then $K_y(x)$ is called the reproducing kernel of $\mathcal{H}$ and Hilbert space $\mathcal{H}$ is called the reproducing kernel space.

Particularly, we choose the reproducing kernel spaces $W_2^m[a,b]$ [16] and $W_2^1[a,b]$ with reproducing kernels $K_y^m(x)$ and $k_y(x)$, respectively. The inner product in $W_2^m[a,b]$ is given by

$$\langle u(x), v(x)\rangle = \sum_{i=0}^{m-1} u^i(0)v^i(0) + \int_a^b u^m(x)v^m(x)\mathrm{d}x, \quad u, v \in W_2^m[a,b]. \tag{11}$$

Instead of using the generalized function $\delta(x)$, we skillfully give the general formula of $K_y^m(x)$ with a new method to different smoothness reproducing kernel space $W_2^m[a,b]$, which is proved to be a $2n-1$ order spline function. The explicit representation formula for calculating the reproducing kernel is given as follows.

Theorem 3.2. *The reproducing kernel of the reproducing space $W_2^m[a,b]$ is*

$$K_y^m(x) = \begin{cases}\displaystyle\sum_{i=0}^{m}\left(\frac{(y-a)^i}{i!} + (-1)^{m-1-i}\frac{(y-a)^{2m-1-i}}{(2m-1-i)!}\right) \times \frac{(x-a)^i}{i!}, & x > y,\\[2ex] \displaystyle\sum_{i=0}^{m}\left(\frac{(x-a)^i}{i!} + (-1)^{m-1-i}\frac{(x-a)^{2m-1-i}}{(2m-1-i)!}\right) \times \frac{(y-a)^i}{i!}, & x \le y.\end{cases} \tag{12}$$

Proof. Expanding $u(x)$ around $x = a$, by Taylor's series expansion, one obtains

$$u(x) = \sum_{k=0}^{m-1} \frac{u^{(k)}(a)}{k!}(x-a)^k + \frac{1}{(m-1)!}\int_a^x (x-y)^{m-1}u^{(m)}(y)\mathrm{d}y. \tag{13}$$

Note that $K^m(x,y) \triangleq K_y^m(x)$. Applying the property of reproducing kernel,

$$\begin{aligned} u(x) &= \langle u(y), K^m(x,y)\rangle \\ &= \sum_{k=0}^{m-1} u^{(k)}(a)\frac{\partial^k}{\partial y^k}K^m(x,y) \\ &\quad + \int_a^x (x-y)^{m-1}\frac{\partial^m}{\partial y^m}K^m(x,y)\mathrm{d}y. \end{aligned} \tag{14}$$

Combing eqs (13) and (14), one can obtain

$$\frac{\partial^k K^m(x,y)}{\partial y^k} = \frac{(x-a)^k}{k!}, \qquad k = 0, 1, \ldots, m-1.$$

For $k = m$, we have

$$\frac{\partial^m K^m(x,y)}{\partial y^m} = \begin{cases} \dfrac{(x-y)^{m-1}}{(m-1)!}, & y < x, \\ 0, & y \geq x. \end{cases}$$

The solution of the equation

$$\frac{\partial^m K^m(x,y)}{\partial y^m} = \frac{(x-y)^{m-1}}{(m-1)!}$$

can be expressed as follows:

$$K^m(x,y) = \sum_{k=0}^{m-1} C_k(y-a)^k + (-1)^m\frac{(x-y)^{2m-1}}{(2m-1)!}.$$

Imposing the conditions

$$\frac{\partial^k K^m(x,y)}{\partial y^k} = \frac{(x-a)^k}{k!}, \qquad k = 0, 1, \ldots, m-1,$$

one can obtain

$$C_k = \left[\frac{(x-a)^k}{k!} + (-1)^{m-k-1}\frac{(x-a)^{2m-1-k}}{(2m-1-k)!}\right]\frac{1}{k!}.$$

Consequently,

$$\begin{aligned} K^m(x,y) = &\sum_{k=0}^{m}\left[\frac{(y-a)^k}{k!} + (-1)^{m-k-1}\frac{(y-a)^{2m-1-k}}{(2m-1-k)!}\right] \\ &\times\frac{(x-a)^k}{k!}, \qquad y < x. \end{aligned}$$

Combining the symmetric property of $K^m(x,y)$, one can obtain the expression of $K^m(x,y)$.

Moreover, when extended to multidimensional space, W and $K_{\mathbf{Y}}(\mathbf{X})$ can be induced by W_2^m and $K_y(x)$ respectively (see [16]).

Now, we choose a countable dense subset $\{\mathbf{X}_i\}_{i=1}^{\infty} \subset \Omega$, and thus, get the two following conclusions. □

PROPOSITION 3.3

Let $\psi_i(\mathbf{X}) = \mathcal{L}^* k_{\mathbf{X}_i}(\mathbf{X}) \in W$, where $\mathcal{L}^*$ is the conjugate operator of $\mathcal{L}$, $\mathcal{L}$ is given in eq. (10). *Then $\psi_i(\mathbf{X}) = \mathcal{L}K_{\mathbf{X}}(\mathbf{X}_i)$.*

Proof. For an arbitrary i, we have

$$\begin{aligned} \psi_i(\mathbf{X}) &= \mathcal{L}^* k_{\mathbf{X}_i}(\mathbf{X}) \\ &= \langle \mathcal{L}^* k_{\mathbf{X}_i}(\cdot), K_{\mathbf{X}}(\cdot)\rangle \\ &= \langle k_{\mathbf{X}_i}(\cdot), \mathcal{L}K_{\mathbf{X}}(\cdot)\rangle \\ &= \mathcal{L}K_{\mathbf{X}}(\mathbf{x}_i). \end{aligned}$$

□

The following proposition comes from [16].

PROPOSITION 3.4

The function system $\{\psi_i\}_1^n$ is linearly independent. Moreover, $\{\psi_i\}_1^{\infty}$ is a complete system in the space W.

Let

$$\varphi_i(\mathbf{X}) = \mathcal{R}_i(K_{\mathbf{X}}(\mathbf{Y})), \qquad i = 1, 2, \ldots, c,$$

where $\mathcal{R}_i$ is given in eq. (1) and

$$\begin{aligned} S^{n+c} = \ &\mathrm{span}\{\psi_1(x), \psi_2(x), \ldots, \\ &\psi_n(x), \varphi_1(x), \varphi_2(x), \ldots, \varphi_c(x)\}. \end{aligned}$$

The projection operator is denoted by $\mathcal{P}_{n+c}\colon W \to S^{n+c}$. Then we obtain Theorem 3.5, which is of great significance to us.

Theorem 3.5. *If u is the solution of eq.* (10), *$\mathcal{P}_{n+c}u$ satisfies the following equations*:

$$\begin{cases} \langle u, \psi_i\rangle = f(\mathbf{X}_i), & i = 1, 2, \ldots, n, \\ \langle u, \varphi_i\rangle = \alpha_i, & i = 1, 2, \ldots, c. \end{cases} \tag{15}$$

Proof. Assume $u(\mathbf{X})$ is a solution of eq. (10). Then we have $\mathcal{L}u(\mathbf{X}) = f(\mathbf{X})$ and thus

$$\begin{aligned} \langle \mathcal{P}_{n+c}u(\cdot), \psi_i(\cdot)\rangle &= \langle u(\cdot), \mathcal{P}_{n+c}\psi_i(\cdot)\rangle \\ &= \langle u(\cdot), \psi_i(\cdot)\rangle \\ &= \langle u(\cdot), \mathcal{L}K_{\mathbf{X}_i}(\cdot)\rangle \\ &= \langle \mathcal{L}u(\cdot), K_{\mathbf{X}_i}(\cdot)\rangle \\ &= \mathcal{L}u(\mathbf{X}_i) \\ &= f(\mathbf{X}_i), \qquad i = 1, 2, \ldots, n; \\ \langle \mathcal{P}_{n+c}u(\cdot), \varphi_i(\cdot)\rangle &= \langle u(\cdot), \mathcal{P}_{n+c}\varphi_i(\cdot)\rangle \\ &= \langle u(\cdot), \varphi_i(\cdot)\rangle \\ &= \langle u(\cdot), R_i(K_{\mathbf{X}}(\cdot))\rangle = R_i\langle u(\cdot), K_{\mathbf{X}}(\cdot)\rangle \\ &= R_i(u(\mathbf{X})) = \alpha_i, \quad i = 1, 2, \ldots, c. \end{aligned}$$

□

In fact, $U^n(\mathbf{X}) \triangleq (\mathcal{P}_{n+c}u)(\mathbf{X})$ is an approximate solution of eq. (10).

Theorem 3.6. *$U^n(\mathbf{X})$ uniformly converges to $u(\mathbf{X})$ on Ω.*

Proof. Note that

$$u(\mathbf{X})=\langle u(\cdot),\, K_{\mathbf{X}}(\cdot)\rangle, \quad U^n(\mathbf{X})=\langle(\mathcal{P}_{n+c}u(\cdot)),\, K_{\mathbf{X}}(\cdot)\rangle.$$

By Schwarz's inequality, we have

$$\begin{aligned}|u(\mathbf{X})-U^n(\mathbf{X})| &= |\langle u(\mathbf{Y})-U^n(\mathbf{Y}),\, K_{\mathbf{X}}(\mathbf{Y})\rangle| \\ &\le \|u(\mathbf{Y})-U^n(\mathbf{Y})\|\|K_{\mathbf{Y}}(\mathbf{Y})\| \\ &= \sqrt{K_{\mathbf{Y}}(\mathbf{Y})}\|u(\mathbf{Y})-U^n(\mathbf{Y})\|.\end{aligned}$$

As $K_{\mathbf{Y}}(\mathbf{Y})$ is continuous on Ω, $|K_{\mathbf{Y}}(\mathbf{Y})| \le M$ and thus we have

$$|u(\mathbf{X})-U^n(\mathbf{X})| \le M\|u-U^n\| \to 0.$$

Hence, $U^n(\mathbf{X}) \rightrightarrows u(\mathbf{X})$, as required. □

As $U^n \in S^{n+c}$, U_n can be expressed in the following form:

$$U^n(\mathbf{X}) = \sum_{i=1}^{n} a_i\psi_i(\mathbf{X}) + \sum_{i=1}^{c} b_i\varphi_i(\mathbf{X}). \tag{16}$$

The n coefficients $a_1,\dots,a_n$ and $b_1,\dots,b_c$ are determined by substituting eq. (16) into eq. (15). In such a manner, one can obtain a system of linear equations:

$$\begin{cases}\displaystyle\sum_{j=1}^{n} a_j\langle\psi_j,\psi_i\rangle + \sum_{j=1}^{c} b_j\langle\psi_i,\varphi_j\rangle = f(\mathbf{X}_i), \\ \qquad i=1,2,\dots,n, \\ \displaystyle\sum_{j=1}^{n} a_j\langle\psi_j,\varphi_i\rangle + \sum_{j=1}^{c} b_j\langle\varphi_i,\varphi_j\rangle = \alpha_i, \quad i=1,2,\dots,c.\end{cases} \tag{17}$$

Let

$$G=\begin{pmatrix}\langle\psi_1,\psi_1\rangle & \langle\psi_1,\psi_2\rangle\dots\langle\psi_1,\psi_n\rangle & \langle\psi_1,\varphi_1\rangle\dots\langle\psi_1,\varphi_c\rangle \\ \vdots & \vdots \quad \vdots \quad \vdots & \vdots \quad \vdots \quad \vdots \\ \langle\psi_n,\psi_1\rangle & \langle\psi_n,\psi_2\rangle\dots\langle\psi_n,\psi_n\rangle & \langle\psi_n,\varphi_1\rangle\dots\langle\psi_n,\varphi_c\rangle \\ \langle\varphi_1,\psi_1\rangle & \langle\varphi_1,\psi_2\rangle\dots\langle\varphi_1,\psi_n\rangle & \langle\varphi_1,\varphi_1\rangle\dots\langle\varphi_1,\varphi_c\rangle \\ \vdots & \vdots \quad \vdots \quad \vdots & \vdots \quad \vdots \quad \vdots \\ \langle\varphi_c,\psi_1\rangle & \langle\varphi_c,\psi_2\rangle\dots\langle\varphi_c,\psi_n\rangle & \langle\varphi_c,\varphi_1\rangle\dots\langle\varphi_c,\varphi_c\rangle\end{pmatrix},$$

$$f = \begin{pmatrix} f(\mathbf{X}_1) \\ \vdots \\ f(\mathbf{X}_n) \\ \alpha_1 \\ \vdots \\ \alpha_c \end{pmatrix}.$$

It is not difficult to prove that the matrix G is reversible. Thus, we have

$$(a_1,a_2,\dots,a_n,b_1,\dots,b_c)^T = G^{-1}f. \tag{18}$$

Consequently, $U^n(\mathbf{X})$ given in eq. (16) can be calculated.

Overall, by applying our new approach, that is, the combination of the HDM and the SRKM, we give the process of obtaining the approximation of the following nonlinear equation:

$$\begin{cases}\mathcal{L}(u)+g(u)=f(\mathbf{X}), & \mathbf{X}\in\Omega \\ \mathcal{R}(u)=\alpha, & \alpha\in R^c,\end{cases} \tag{19}$$

where $\mathcal{L}$ is linear and g is nonlinear.

(1°) Construct $\psi_i, i=1,2,\dots,n$ and $\varphi_i, i=1,2,\dots,c$, then compute G.

(2°) $p^k: \mathcal{L}u_k=f_k, \mathcal{R}u_k=\alpha/2^{k+1}$, for $k=0,1,\dots$. Compute the $n+c$ coefficients $(a_{k1},a_{k2},\dots,a_{kn},b_{k1},b_{k2},\dots,b_{kc})^T = G^{-1}f_k$ and get a n-term approximation:

$$U_k^n(\mathbf{X}) = \sum_{i=1}^{n} a_{ki}\psi_i(\mathbf{X}) + \sum_{i=1}^{c} b_{ki}\varphi_i(\mathbf{X}). \tag{20}$$

(3°) Get the m-term approximation $U_{m,n}(\mathbf{X})$ of eq. (19),

$$U_{m,n}(\mathbf{X}) = \sum_{k=0}^{m} U_k^n(\mathbf{X}). \tag{21}$$

4. Numerical examples

In this section, some higher-order nonlinear differential equations are considered to reveal the accuracy of our algorithm. Compared with refs [12] and [17], the results obtained demonstrate that our algorithm is remarkably effective for the following numerical examples.

Example 4.1. Consider the three-point BVP for the second-order nonlinear differential equation presented in [17]:

$$\begin{cases}u''(x)+(3/8)u(x)+(2/1089)[u'(x)]^2+1=0, \\ \quad x\in[0,1], \\ u(0)=0, \qquad u(1/3)=u(1).\end{cases}$$

Following the present method, we take $m=3$ and $n=3$, 10 and 50, and we obtain the approximation $U_{m,n}(x)$ of $u(x)$. As the exact solution $u(x)$ of this problem is unknown, we instead consider $e_{m,n}(x)$ with

$$e_{m,n}(x) = U''_{m,n}(x)+\frac{3}{8}U_{m,n}(x)+\frac{2}{1089}[U'_{m,n}(x)]^2+1. \tag{22}$$

In table 1, some values of $e_{m,n}(x)$ are illustrated for some values of x. By comparing our values with the values of $e_{m,n}(x)$ obtained by different method [17], we

Table 1. Comparison of some methods for Example 4.1.

x_i	$e_{3,10}$	$e_{3,50}$	Method in [17]
0.2	3.87×10^{-10}	7.77×10^{-11}	2.58×10^{-11}
0.4	4.68×10^{-10}	2.08×10^{-12}	4.31×10^{-10}
0.6	4.42×10^{-10}	6.11×10^{-11}	9.91×10^{-9}
0.8	4.08×10^{-10}	1.24×10^{-10}	9.12×10^{-8}

found that our method is in good agreement with other methods.

Example 4.2. Consider the two-point BVP for the third-order nonlinear differential equation with a radical nonlinearity proposed in [12].

$$\begin{cases} u'''(x) = -\sqrt{1-u^2(x)}, & 0 \le x \le (\pi/2), \\ u(0) = 0, \quad u'(0) = 1, & u(\pi/2) = 1. \end{cases} \tag{23}$$

By Example 2 of [12], its exact solution is $u(x) = \sin(x)$. Applying our new method, we take $m = 2, 4, 6, 8, 12$ and $n = 50$, the absolute error $ME_n = |u(x) - U_{m,n}(x)|_{\max}$ is listed in table 2. At the same time, one can see that the new method is much more accurate from the comparison given in table 2. When we take $m = 3, 5, 8$ and $n = 100$, the absolute errors $|u(x) - U_{m,n}(x)|$ between the approximate solution and exact solution are given in figure 1.

Example 4.3. Consider the four-point BVP for the fourth-order nonlinear differential equation with a product nonlinearity shown in [12].

$$\begin{cases} u''''(x) + u(x)u'(x) - 4x^7 - 24 = 0, \quad x \in [0, 1], \\ u(0) = 0, \quad u'''(0.25) = 6, \quad u''(0.5) = 3, \quad u(1) = 1. \end{cases}$$

By Example 4 of [12], its exact solution is $u(x) = x^4$. When we take $m = 3$ and $n = 2, 3, 4, 5$ and 10, the absolute errors $ME_n = |u(x) - U_{m,n}(x)|$, $ME'_n = |u'(x) - U'_{m,n}(x)|$, $ME''_n = |u''(x) - U''_{m,n}(x)|$ are

Table 2. Comparison of some methods for Example 4.2.

m	2	4	6	8	12
New method	0.004839	0.000036	5.03×10^{-6}	4.64×10^{-6}	3.73×10^{-6}
Method in [12]	0.024046	0.004132	0.00182015	0.00103552	0.00047603

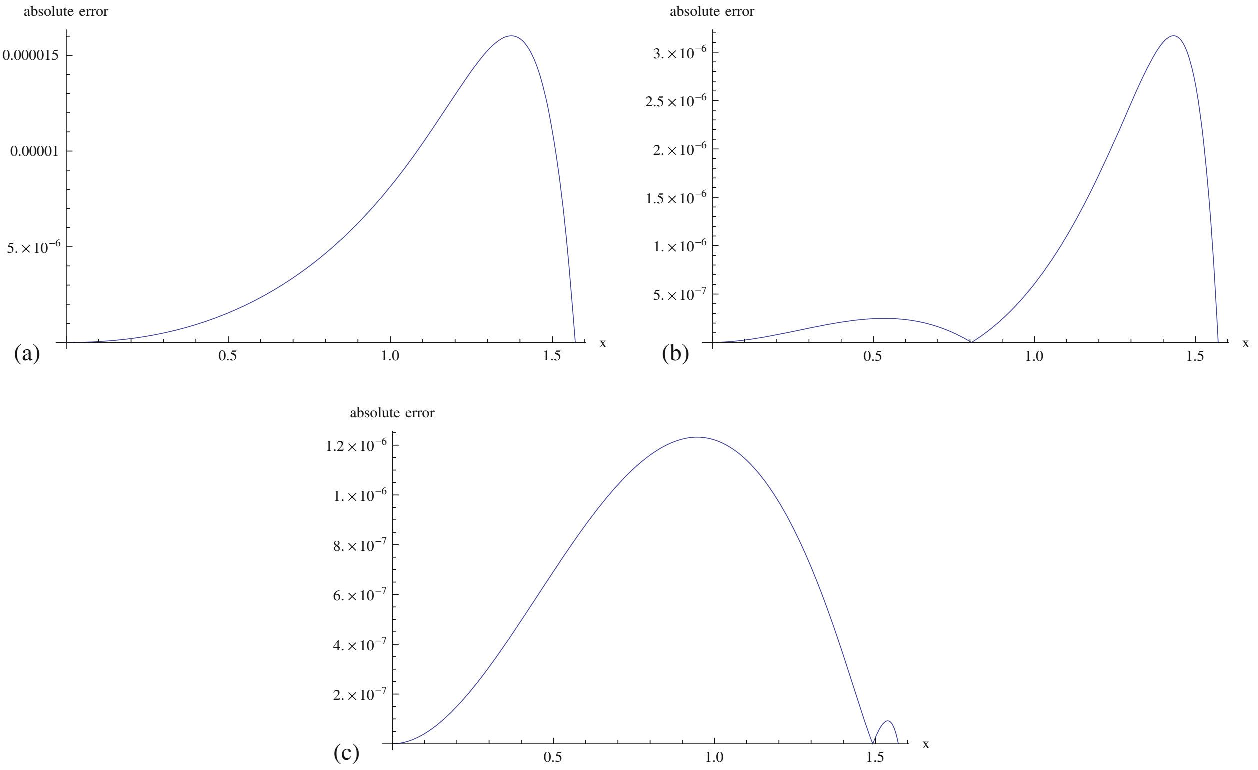

Figure 1. (**a**) $|u(x) - U_{3,100}(x)|$, (**b**) $|u(x) - U_{5,100}(x)|$ and (**c**) $|u(x) - U_{8,100}(x)|$.

shown in table 3. From the table, one can see that the absolute error ME_n reduces to 10^{-14} as $n = 4$, which is much more accurate than the result, 10^{-9}, presented in Example 4 of [12]. Besides, ME_n', ME_n'' decline to 10^{-13} and 10^{-12}, respectively. When we take $m = 2, 3, 4$ and $n = 4$, the absolute errors $|u(x) - U_{m,n}(x)|$ between the approximate solution and exact solution are given in figure 2.

Example 4.4. Consider the following second-order nonlinear partial differential equation:

$$\begin{cases} \dfrac{\partial^2 u}{\partial x^2} - \dfrac{\partial u}{\partial t} - u^2(x,t) = f(x,t), \quad x \in [0, 1], t \in [0, 1], \\ u(0, t) = 0, \quad t \in [0, 1], \\ u(1, t) = \sin(t), \quad t \in [0, 1], \\ u(x, 0) = 0, \quad x \in [0, 1]. \end{cases}$$

Table 3. Numerical result for Example 4.3.

n	2	3	4	5	10
ME_n	4.5×10^{-9}	1.4×10^{-11}	5.6×10^{-14}	4.0×10^{-16}	3.5×10^{-16}
ME_n'	1.5×10^{-8}	5.1×10^{-11}	2.2×10^{-13}	5.0×10^{-15}	4.0×10^{-15}
ME_n''	2.0×10^{-7}	4.5×10^{-10}	2.0×10^{-12}	1.5×10^{-14}	1.4×10^{-14}

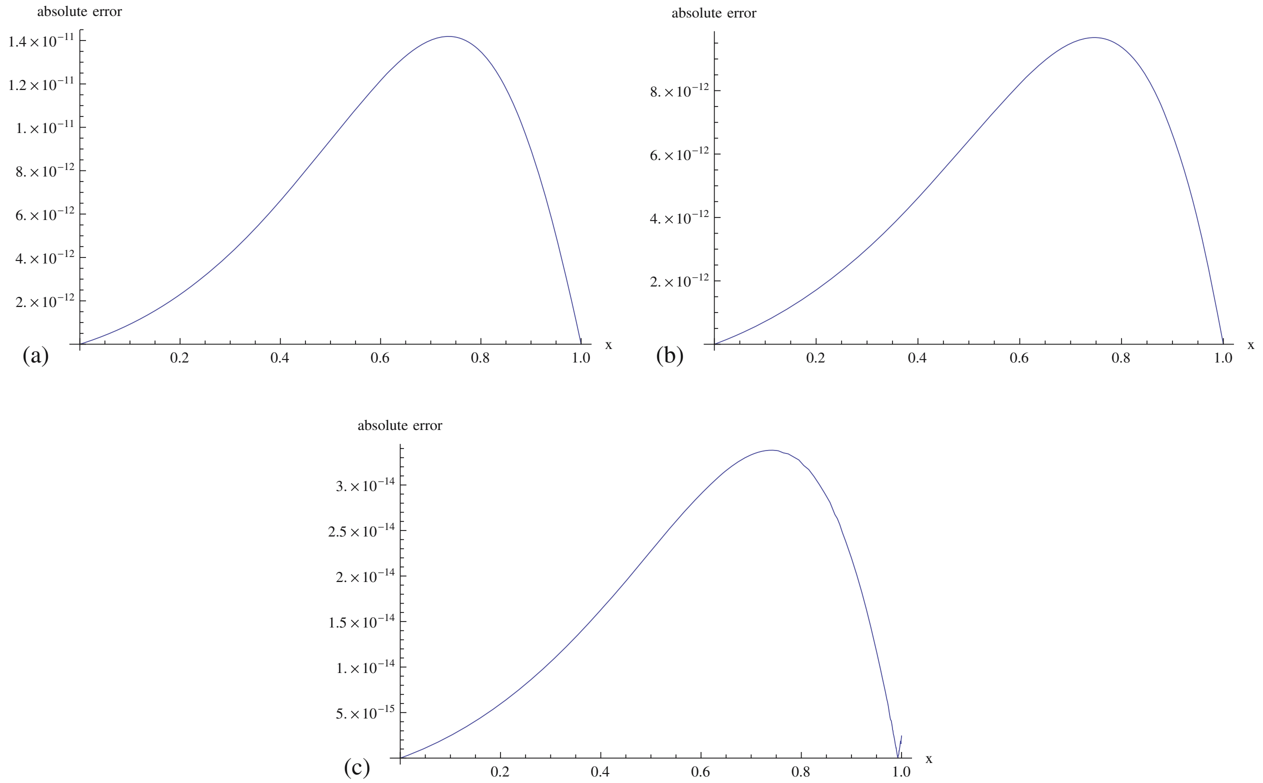

Figure 2. (**a**) $|u(x) - U_{2,4}(x)|$, (**b**) $|u(x) - U_{3,4}(x)|$ and (**c**) $|u(x) - U_{4,4}(x)|$.

Table 4. Numerical values and error analysis of Example 4.4.

Node	$u(x,t)$	$U_{3,100}(x,t)$	$U_{3,200}(x,t)$	$\lvert u(x,t) - U_{3,100}(x,t)\rvert$	$\lvert u(x,t) - U_{3,200}(x,t)\rvert$
(0.1, 0.1)	0.00999983	0.00999521	0.0099994	4.6×10^{-6}	4.3×10^{-7}
(0.3, 0.3)	0.0898785	0.0899523	0.0898916	7.4×10^{-5}	1.3×10^{-5}
(0.5, 0.5)	0.247404	0.247576	0.247432	1.7×10^{-4}	2.8×10^{-5}
(0.7, 0.7)	0.470626	0.47079	0.470654	1.6×10^{-4}	2.8×10^{-5}
(0.9, 0.9)	0.724287	0.724338	0.724296	5.1×10^{-5}	8.7×10^{-6}

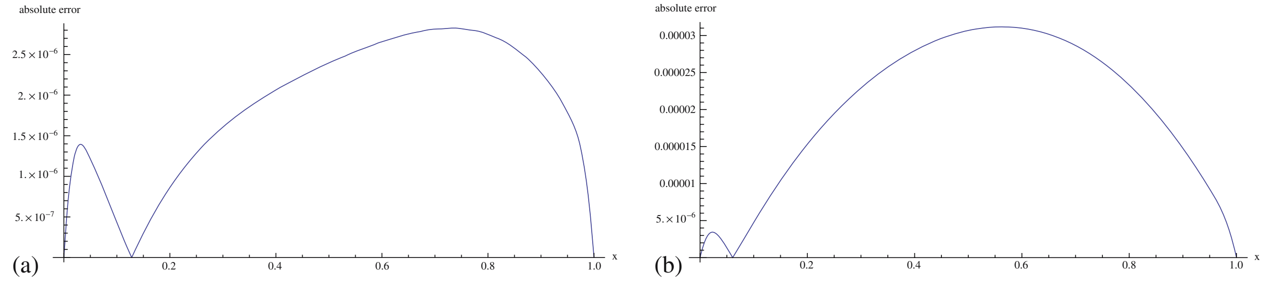

Figure 3. (**a**) $|u(x, 0.1) - U_{3,200}(x, 0.1)|$ and (**b**) $|u(x, 0.6) - U_{3,200}(x, 0.6)|$.

When $f(x,t) = -x\cos(xt) - t^2\sin(xt) - \sin^2(xt)$, its exact solution is $u(x,t) = \sin(xt)$. Applying this method, we take $m = 3$, $n = 10 \times 10$ and $n = 20 \times 20$ nodes in $\Omega = [0, 1] \times [0, 1]$ to obtain the approximation $U_{m,n}(x,t)$. Some values of exact and numerical solution of some nodes as well as the errors between them are given in table 4. One can see that the errors reduce as nodes increase. When $m = 3$ and $n = 200$, the absolute errors $|u(x,t) - U_{m,n}(x,t)|$ are given in figure 3.

5. Conclusion

From the above analysis and the numerical examples, one can see that the combination of the HDM and the SRKM is employed successfully for solving higher-order nonlinear complicated BVPs. The numerical results show that our algorithm is much more accurate than other algorithms.

References

[1] F Wong and W Lian, *Comput. Math. Appl.* **32**, 41 (1996)
[2] S Chen, W Ni and C Wang, *Appl. Math. Lett.* **19**, 161 (2006)
[3] C Bai, D Yang and H Zhu, *Appl. Math. Lett.* **20**, 1131 (2007)
[4] A Ravi Kanth and K Aruna, *Phys. Lett. A* **372**, 4671 (2008)
[5] Y Zhong, S Chen and C Wang, *Appl. Math. Lett.* **21**, 465 (2008)
[6] Y Liu and H Yu, *Comput. Math. Appl.* **50**, 133 (2005)
[7] T He, F Yang, C Chen and S Peng, *Comput. Math. Appl.* **61**, 3355 (2011)
[8] F Geng, *Appl. Math. Comput.* **215**, 2095 (2009)
[9] J S Duan, *Appl. Math. Comput.* **217**, 6337 (2011)
[10] M Tatari and M Dehghan, *Phys. Scri.* **73**, 672 (2006)
[11] F Geng and M Cui, *Int. J. Nonlin. Sci. Num.* **10**, 597 (2009)
[12] J Duan and R Rach, *Appl. Math. Comput.* **218**, 4090 (2011)
[13] S Abbas and D Mehdi, *Commun. Nonlinear Sci. Numer. Simul.* **17**, 593 (2012)
[14] Shijun Liao, *Commun. Nonlinear Sci. Numer. Simul.* **2**, 95 (1997)
[15] Y Lin and J Lin, *Commun. Nonlinear Sci. Numer. Simul.* **15**, 3855 (2010)
[16] Minggen Cui and Y Lin, *Nonlinear numerical analysis in the reproducing kernel space* (Nova Science Publishers, Inc, 2008)
[17] M Tatari and M Dehghan, *J. Vib. Control* **18**, 1116 (2012)